



## DAMAGE EVALUATION OF PRESTRESSED CONCRETE BEAMS POST-TENSIONED WITH UNBONDED TENDONS

H. Watanabe<sup>(1)</sup>, S. Kono<sup>(2)</sup>, T. Obara<sup>(3)</sup>, L. Martinelli<sup>(4)</sup>, G. Gioia<sup>(5)</sup>

<sup>(1)</sup> Assistant Professor, Urban Disaster Prevention Research Core, Tokyo Institute of Technology, watanabe.h.as@m.titech.ac.jp

<sup>(2)</sup> Professor, Urban Disaster Prevention Research Core, Tokyo Institute of Technology, kono.s.ae@m.titech.ac.jp

<sup>(3)</sup> Graduate student, Dep. of Architecture and Building Engineering, Tokyo Institute of Technology, obara.t.ac@serc.titech.ac.jp

<sup>(4)</sup> Associate Professor, Dep. of Civil and Environmental Engineering, Politecnico di Milano, luca.martinelli@polimi.it

<sup>(5)</sup> Professional Engineer, gianluca.gioia@outlook.com

### Abstract

In major earthquake, many reinforced concrete buildings were damaged. Some of the buildings had severe economical losses due to structural or nonstructural damage until after the rehabilitation has been completed, even though the buildings did not collapse. For this reason, demand level for structural design shifted to be higher in Japanese society. In order to develop such high performance buildings, this study focuses on the unbonded prestressing structures as self-centering system. The structures are able to sustain seismic force with small residual deformation. In PRESS research program, a hybrid system with self-centering system and energy dissipation devices was developed. The small residual deformation and structural performance of the hybrid system were confirmed by structural tests. However, few studies have been reported on evaluating damage after earthquake for the unbonded prestressing structures. In order to fully take advantage of low damage characteristics of the self-centering system, it is important to investigate structural performance and damage after the earthquakes. Thus, this study reports on evaluating damage of post-tensioned precast concrete members.

In order to investigate effect of effective prestressing force ratio and shear span ratio on damage or hysteresis characteristics, four specimens were made. A specimen was designed to investigate structural performance of a repaired beam after an earthquake. The structural experiment was conducted using the specimens under cyclic static loading. As an experimental result, small residual drift angle is observed of all specimens. The Shear force versus drift angle responses had S-shape hysteresis behavior which has small amount of energy dissipation.

The 2015 AIJ prestressed concrete guidelines define four limit states (Serviceability limit state, Reparability limit state I, Reparability limit state II and Safety limit state) and damage evaluation criteria for the limit states. Damage evaluation was conducted using the experimental results and these criteria. As an evaluation result, effective prestressing force ratio is one of important factors in order to control damage in design for unbonded prestressed concrete beams. Furthermore, except for one specimen, the drift angle at serviceability limit state ranged from  $R=0.5\%$  to  $R=1.0\%$ . All specimens did not reach safety limit state until  $R=4\%$ . Thus, excellent low damage performances of unbonded prestressed concrete beams were confirmed.

*Keywords: prestressed concrete beams; unbonded tendon; damage evaluation; limit state*



## 1. Introduction

In the 1995 Kobe Earthquake and the 2011 Tohoku Earthquake, many reinforced concrete buildings were damaged. Some of the buildings had severe economical losses due to structural or nonstructural damage until after the rehabilitation has been completed, even though the buildings did not collapse. For this reason, demand level for structural design shifted to be higher in Japanese society. In the case of structural design for important structures, no or minimal damage of structure is required even if after huge earthquake.

In order to develop such high performance buildings, this study focuses on the unbonded prestressing structures as self-centering system. Unbonded prestressed concrete structures have been attracting attention in terms of their excellent low damage performances. They consist of precast members which are connected together through unbonded post-tensioning tendons. Deformation of the members is lumped at the connection through opening and closing of an existing gap at the interface. The members may open in the connection for large scale earthquakes but opening tends to close due to the prestressing force. Thus, they are able to sustain seismic force with small residual deformation.

Hybrid structure with precast post-tensioned concrete frame and energy dissipation devices was developed as a product in PRESS (PREcast Seismic Structural Systems) research program<sup>[1][2][3]</sup>. Beams of this structure are connected to columns by unbonded post-tensioning. Mild steel reinforcing bars are placed in top and bottom of beams to dissipate energy by yielding. Those were through corrugated ducts in the beams and columns. The performance of the system was good, with damage being limited to minor spalling of cover concrete in the beams. Furthermore, the residual drift after the loading is very small (0.06 percent). One of the applications is Paramount building<sup>[4]</sup> (39-stories apartment building in San Francisco). However, the system developed in PRESS has complex beam section, because the mild steel reinforcing bars and prestressing tendons are located at the same section. Marriott et al. developed a simpler system by placing the energy dissipation devices outside the critical section<sup>[5]</sup>. In this system, self-centering system and energy dissipation devices developed separately.

The small residual deformation and structural performance of the hybrid system were confirmed by existing researches. However, few studies have been reported on evaluating damage after earthquake for the unbonded prestressing structures. In order to fully take advantage of low damage characteristics of self-centering system, it is important to investigate structural performance and damage after the earthquakes. Thus, this study focuses on evaluating damage of post-tensioned precast concrete members.

## 2. Experimental program

### 2.1 specimen details

Five specimens (PCa11-15) in Table 1 were tested. They are precast concrete beams post-tensioned with unbonded tendons. Figure 1 shows reinforcement details. All specimens had identical details except diameter of prestressing tendon. The specimens were 1/2 scale models. Beam width and depth are 500mm and 600mm, respectively. The longitudinal mild reinforcement was placed to assemble shear reinforcement. Therefore, those were curtailed at the ends of the beams. The distance between the stub face and the loading point was 3300mm for PCa12 and that for the other specimens was 1800mm. Prestressing tendons were located in corrugated steel sheaths with 50mm internal diameter. Beams and stubs were cast separately and connected using four unbonded prestressing tendons after placing non-shrinkage joint mortar between them. In order to measure force of the prestressing tendons, a load cell was placed at the stub end of each prestressing tendon. Eighty percent of yield strength was introduced to tendons as effective prestress. Measured forces of prestressing tendons are shown in Table 1. All specimens were designed to fail in flexure. The material properties of the specimens are shown in Table 2 and Table 3.

Prototype specimen PCa3 is a prestressed half-precast concrete beam<sup>[6]</sup>. In order to investigate effects of effective prestressing force ratio and shear span ratio on damage or hysteresis characteristics, PCa11, PCa12, PCa13 and PCa14 were made. PCa15A were designed to investigate structural performance of a repaired beam after an earthquake. PCa15A was loaded until drift angle  $R=2.0\%$ ; thereafter, PCa15A is repaired using mortar after removing damaged concrete. In this paper, repaired PCa15A is called as PCa15B, hereafter.

Shear force was applied by a vertical hydraulic jack as shown in Fig. 1. The cyclic loading protocol is



shown in Fig. 2. The loading protocol consisted of two cycles at drift angle  $R=0.125\%$ ,  $0.25\%$ ,  $0.5\%$ ,  $1.0\%$ ,  $1.5\%$ ,  $2.0\%$ ,  $3.0\%$ ,  $4.0\%$  and one cycle at drift angles of  $R=0.5\%$  after  $R=1.0\%$  and  $R=2.0\%$  to investigate the inner loop.

Table 1 – Specifications of the specimens

Specimen	PCa3	PCa11	PCa12	PCa13	PCa14	PCa15A (before repair)	PCa15B (after repair)
Specified concrete compressive strength	60MPa			30MPa	100MPa + steel fiber *2	60MPa	
Beam	Width (B)						
	Depth (D)						
	Longitudinal mild reinforcement						
	4- $\phi$ 32		4- $\phi$ 23		4- $\phi$ 32		
	Sheath						
	Shear reinforcement						
shear span ratio	3.0		5.5	3.0			
Prestressing factor ( $\lambda$ )	1.0						
effective prestressing force ratio ( $\eta$ ) *1	0.16	0.07	0.13	0.25	0.09	0.13	0.13
Total initial prestressing force (P)	2859kN	1468kN	2818kN	2709kN	2774kN	2719kN	2719
comment	standard	Low PC force	large shear span ratio	Low f <sub>c</sub>	High f <sub>c</sub>	Repaired	

\*1  $\eta = P/(f_c \cdot B \cdot D)$

where, P is total initial prestressing force, f<sub>c</sub> is concrete compressive strength, B is beam width and D is beam depth

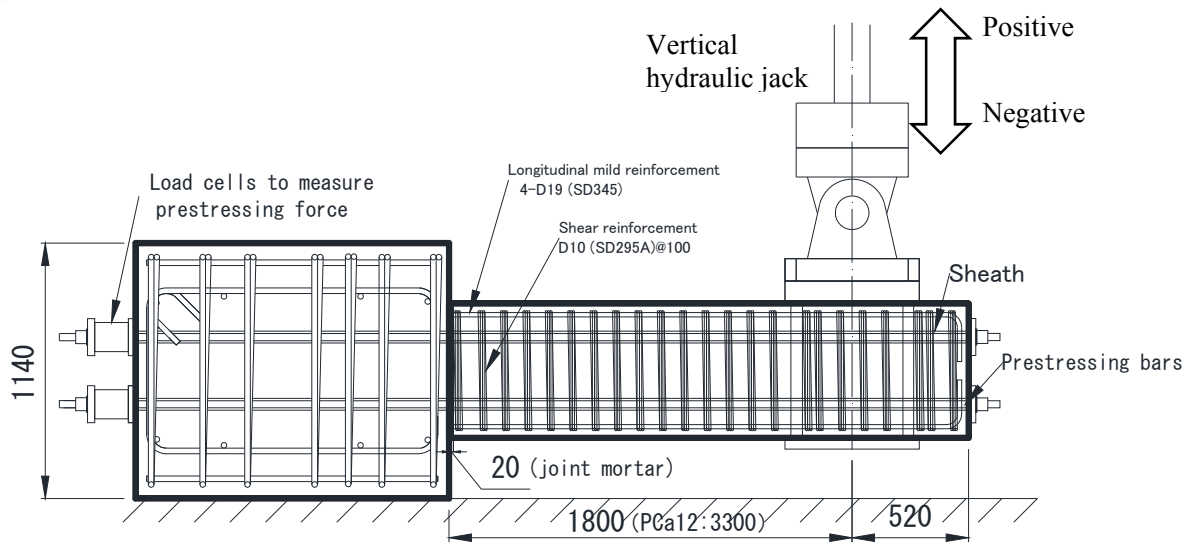
\*2 Steel fiber had diameter:0.62(mm), length:30(mm), aspect ratio:48, tensile strength:1080(Mpa), volume ratio:0.5% and end hooks.

Table 2 – Material properties

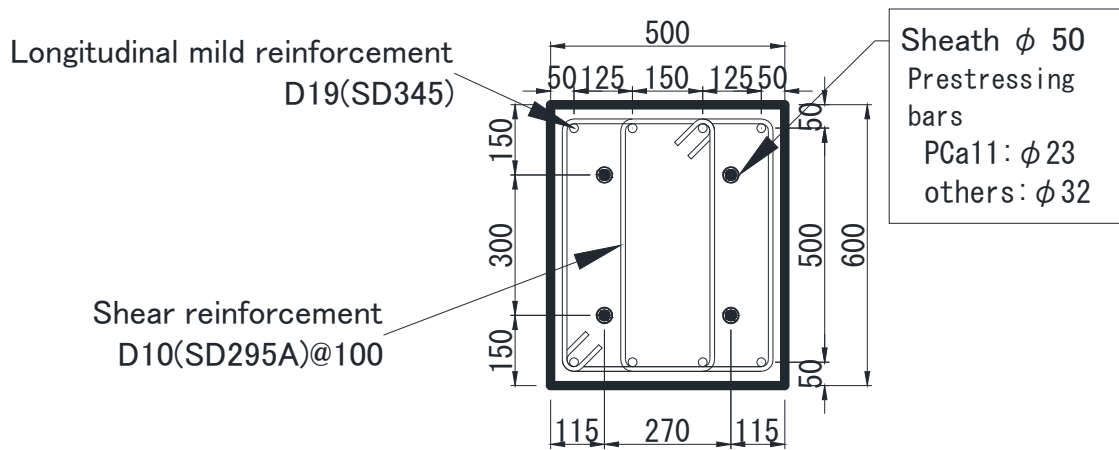
	Diameter	Specimen	Grade	Yield stress (MPa)	Strain at yield stress (%)	Tensile strength (MPa)	Young's modulus (GPa)
Longitudinal mild reinforcement	D19	All specimens	SD345	375	0.202	555	186
Shear reinforcement	D10	All specimens	SD295A	371	0.204	545	182
Prestressing bar	$\phi$ 23	PCa11	C-1	1184*	0.808*	1274	190
	$\phi$ 32	PCa12-15	C-1	1150*	0.789*	1263	193

\*0.2% offset yield stress

Specimen	Beam concrete			Joint mortar			Repairing mortar		
	Compressive strength f <sub>c</sub> (MPa)	Young's modulus (GPa)	Splitting tensile strength f <sub>t</sub> (MPa)	Compressive strength f <sub>c</sub> (MPa)	Young's modulus (GPa)	Splitting tensile strength f <sub>t</sub> (MPa)	Compressive strength f <sub>c</sub> (MPa)	Young's modulus (GPa)	Splitting tensile strength f <sub>t</sub> (MPa)
PCa11	70.1	37.9	3.7	112	37.0	4.3			
PCa12	70.1	36.9	4.0	86.7	33.0	4.7			
PCa13	35.7	29.9	2.9	119	38.3	4.3			
PCa14	105	42.4	5.3	105	36.9	4.7			
PCa15A	69.7	36.6	3.8	107	33.6	5.8			
PCa15B	78.7	36.9	4.4	112	37.4	3.8	63.4	26.7	3.3



(a) elevation view



(b) Beam section

Fig. 1 – Reinforcement details and test setup

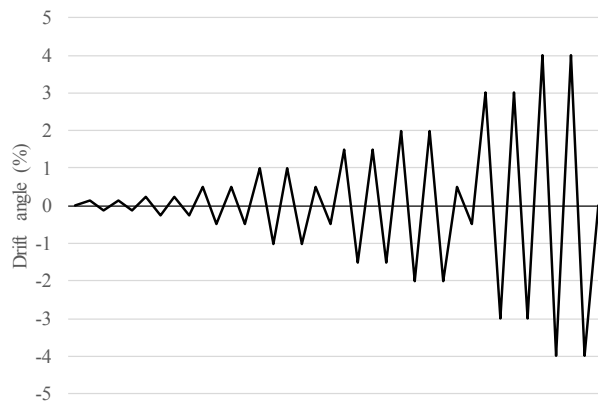


Fig. 2 – Loading protocol

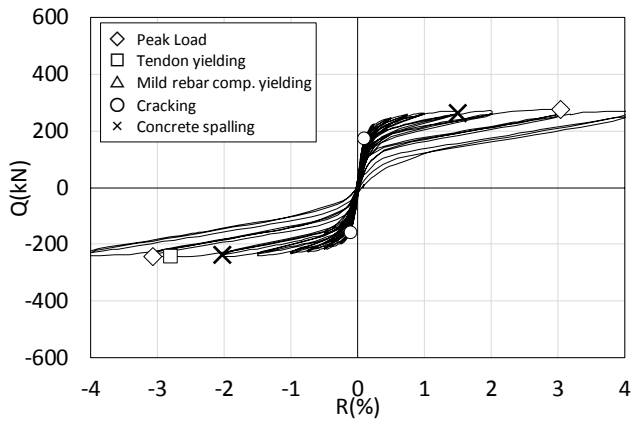


## 2.2 Experimental results

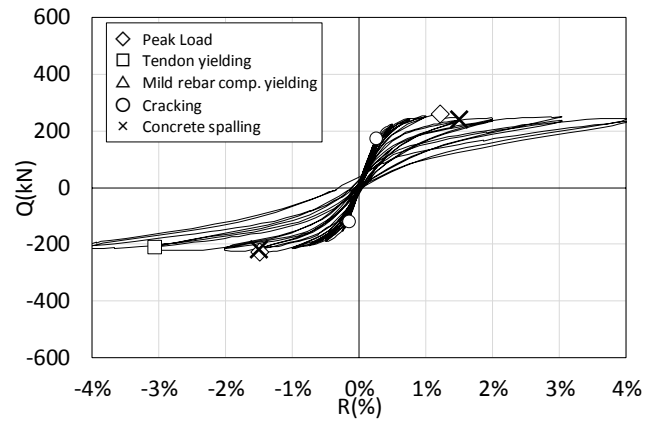
The experimental results are summarized in Table 3. Figure 3 shows shear force (Q) - drift angle (R) responses. Specimens PCa15A and 15B are shown as two specimens. Important response points (peak load, tendon yielding, longitudinal mild reinforcement compressive yielding, cracking, concrete spalling) are plotted. The peak load is recorded between R = 1.0% and R = 3.0% in all specimens. After 1.0%, shear force capacity remains almost constant until 4.0%. Furthermore, small residual drift angle is observed characteristically. At the peak load, deformation of specimen concentrates at a gap between the stub and beam. The gap tended to close due to the prestressing force once unloaded. The Q-R responses had S-shape hysteresis behavior which has small amount of energy dissipation. After tendon yielding, the prestressing force of tendon was reduced from initial force when shear force was 0. Therefore, the negative peak load did not reach the positive peak load. As shown in Table3, compressive yielding of longitudinal mild reinforcement was observed in several specimens. The longitudinal mild reinforcement was curtailed at the beam ends, and, the reinforcement carried only compressive stress. The results show that it is necessary to consider compressive stress of longitudinal mild reinforcement for moment calculation.

Table 3 – Test results

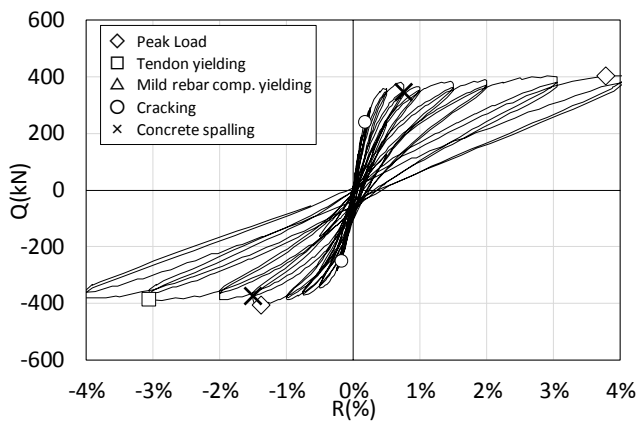
Specimen		Cracking		Concrete spalling		Tendon yielding		Mild rebar comp. yielding		Peak load	
		Q(kN)	R (%)	Q(kN)	R (%)	Q(kN)	R (%)	Q(kN)	R (%)	Q(kN)	R (%)
PCa11	Positive	173	0.10	263	1.50	-	-	-		276	3.05
	Negative	-156	-0.10	-237	-2.02	-244	-2.80			-245	-3.06
PCa12	Positive	173	0.26	239	1.50	231	4.08	248	1.44	259	1.22
	Negative	-118	-0.16	-217	-1.50	-211	-3.06	-213	-1.49	-229	-1.49
PCa13	Positive	241	0.17	346	0.76	404	3.78	380	1.32	404	3.78
	Negative	-251	-0.18	-374	-1.50	-387	-3.06	-377	-1.74	-406	-1.38
PCa14	Positive	314	0.14	483	1.50	512	2.98	481	1.98	512	2.98
	Negative	-284	-0.14	-457	-1.55	-472	-2.82	-459	-3.07	-472	-2.01
PCa15A	Positive	226	0.19	442	1.70	-	-	434	1.69	461	1.90
	Negative	-250	-0.18	-434	-1.60	-	-	-423	-1.59	-443	-2.03
PCa15B	Positive	186	0.14	433	2.00	-	-	410	1.92	469	3.03
	Negative	-145	-0.10	-436	-3.06	-433	-3.67	-412	-1.88	-440	-3.02



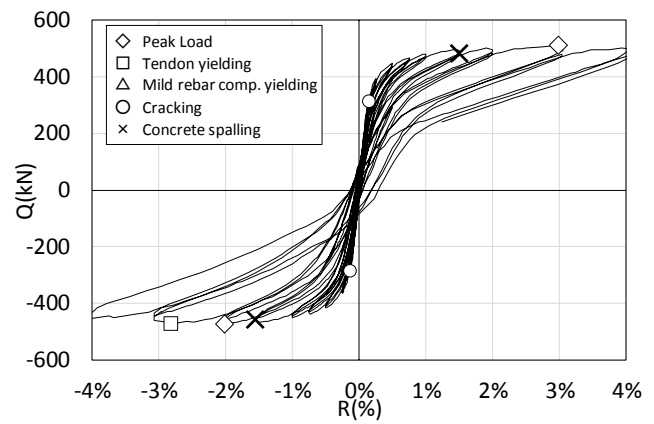
(a) PC11



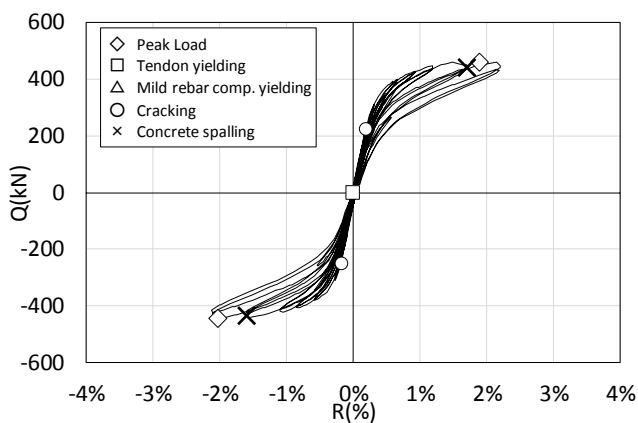
(b) PC12



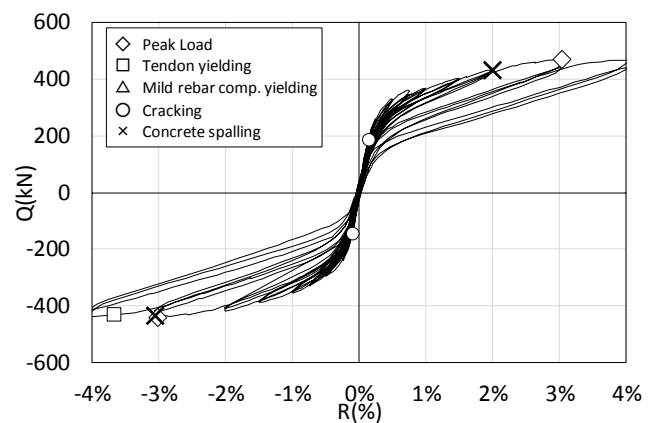
(c) PC13



(d) PC14



(e) PC15A



(f) PC15B

Fig. 3 – Shear force versus drift angle relations

### 3. Damage evaluation

#### 3.1 Method of damage evaluation

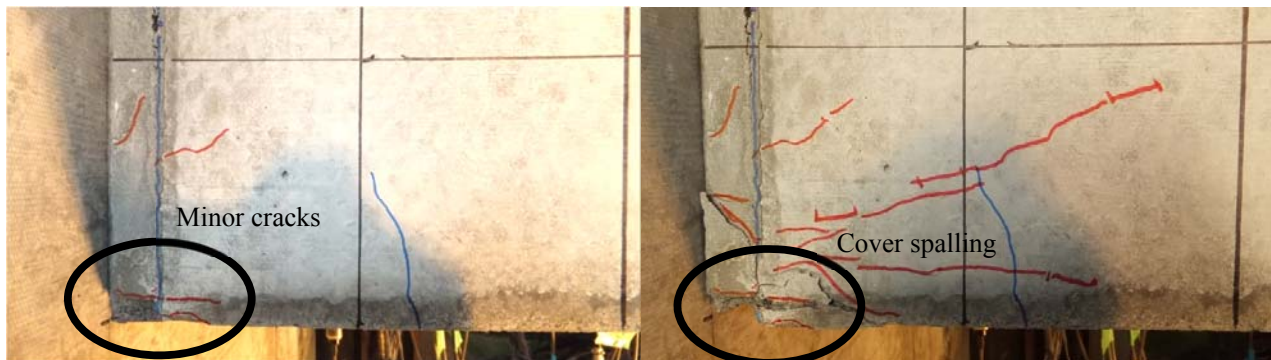
Damage evaluation was conducted using the 2015AIJ prestressed concrete guidelines<sup>[7]</sup>. The guidelines define four limit states (Serviceability limit state, Reparability limit state I, Reparability limit state II and Safety limit state) as shown in Table 4. Limit states were assessed by damage states of concrete, PS tendon and longitudinal mild reinforcement, residual crack width and residual drift angle. Furthermore, our research group added detailed descriptions as shown inside parentheses.

PS tendon was assumed elastic when its strain is less than 0.02 %. PS tendon and longitudinal mild reinforcement were assumed to reach the condition “Yielding is allowed to some extent” when their strain is less than the yield strain. Longitudinal mild reinforcement was assumed to reach the condition “Yielding is allowed” when its strain is less than 1.0 %. Buckling and fracture are judged by photograph. For the concrete, minor cracks in axial direction, spalling of cover concrete and crushing of core concrete are judged from photograph. Two damage are shown in Fig. 4. Serviceability limit of concrete reached when concrete stress reaches  $0.9 f'c$ . Firstly, compressive strain of cover concrete was computed using displacement transducer located on 300mm range from beam-stub interface. Then, compressive stress of cover concrete can be calculated using the strain and strain-stress curve by material test. Residual crack width is measured at each unloading point using PI-shape displacement gauges placed over crack.

Table 4 – Criteria of limit states for flexural members from the 2015 AIJ prestressed concrete guidelines<sup>[7]</sup>

Limit state	Structural performance levels	Longitudinal mild reinforcement	unbonded PS tendons	concrete	Residual drift ratio	Residual crack width
Serviceability limit state	(Immediate occupancy)	Yielding is allowed to some extent (less than yield strain)		less than $0.9f_c$	Nearly 0 ( $R < 0.1\%$ )	less than 0.2mm
Reparability limit state I	(Reparability I)	Yielding is allowed (less than 1.0%)	Elastic (less than 0.02% offset strain)	minor crushing of cover concrete is allowed (minor cracks in axial direction due to compression)	less than 1/400	less than 1.0mm
Reparability limit state II	(Reparability II)	Buckling (Visual judgment from photos)	Yielding is allowed to some extent (less than 0.2% yield strain)	core concrete is intact (cover spalling is allowed)	less than 1/200	less than 2.0mm
Safety limit state	(Life safety)	Fracture (Visual judgment from photos)	Yielding is allowed (Visual judgment from photos)	crushing of core concrete is not observed (Visual judgment from photos)	Drift: less than 4.0%	
	(Collapse prevention)		Fracture	crushing of core concrete	Drift: equal to or more than 4.0%	

\* ( ) inside parentheses are criteria in our research group. They are not parts of the guidelines.



(a) Minor cracks in axial direction due to compression

(b) Spalling of cover concrete

Fig. 4 – Example of concrete damage (PCa11; bottom of the beam under the negative peak)



### 3.2 Results of damage evaluation

Damage evaluation results are shown in Table 5. Drift angles at each limit state were determined by the minimum drift in each column. In all specimens and all limit states, concrete damage was the determinant factor of the limit states as shown in grayed values. PCa13 which has high effective prestressing force ratio had serviceability limit state:  $R=+0.27\%$ , reparability limit state I:  $R=+0.64\%$ , reparability limit state II:  $R=+0.76\%$ , respectively. The drifts are small compared with other specimens. On the other hand, PCa11 which has low effective prestressing force ratio had serviceability limit state:  $R=+0.93\%$ , reparability limit state I:  $R=+0.99\%$ , reparability limit state II:  $R=+1.50\%$  respectively. The drifts are large compared with other specimens. As the effective prestressing force ratio increased, the drift angles at each limit state became small. These results suggest that effective prestressing force ratio is one of important factors in order to control damage in design for unbonded prestressed concrete beams.

Except for PCa13, which has high effective prestressing force ratio, the drift angle at serviceability limit state ranged from  $R=0.5\%$  to  $R=1.0\%$ . Furthermore, all specimens did not reach the safety limit state until  $R=4\%$ . Thus, excellent low damage performances of unbonded prestressed concrete beams was confirmed.

Table 5 – drift angles at each limit states

PCa11	Serviceability limit state		Reparability limit state I		Reparability limit state II		Safety limit state	
	Positive	Negative	Positive	Negative	Positive	Negative	Positive	Negative
Longitudinal mild reinforcement	-	-	-	-	-	-	-	-
Unbonded PS tendons			2.31%*	-1.67%	-*	-2.80%	-	-
Concrete	0.93%	-0.85%	0.99%	-1.00%	1.50%	-2.02%	-	-
Residual drift ratio	-	-	-	-	-	-	-	-
Residual crack width	-	-	-	-	-	-	-	-
The minimum drift	0.93%	-0.85%	0.99%	-1.00%	1.50%	-2.02%	-	-

PCa12	Serviceability limit state		Reparability limit state I		Reparability limit state II		Safety limit state	
	Positive	Negative	Positive	Negative	Positive	Negative	Positive	Negative
Longitudinal mild reinforcement	1.44%	-1.49%	-	-	-	-	-	-
Unbonded PS tendons			1.98%	-1.59%	4.08%	-3.06%	-	-
Concrete	0.67%	-0.69%	0.98%	-0.99%	1.50%	-1.50%	-	-
Residual drift ratio	-	-	-	-	-	-	-	-
Residual crack width	-	-	-	-	-	-	-	-
The minimum drift	0.67%	-0.69%	0.98%	-0.99%	1.50%	-1.50%	-	-

PCa13	Serviceability limit state		Reparability limit state I		Reparability limit state II		Safety limit state	
	Positive	Negative	Positive	Negative	Positive	Negative	Positive	Negative
Longitudinal mild reinforcement	1.32%	-1.74%	-	-	-	-	-	-
Unbonded PS tendons			2.50%	-1.88%	3.78%	-3.06%	-	-
Concrete	0.27%	-0.28%	0.64%	-0.75%	0.76%	-1.50%	-	-
Residual drift ratio	3.06%	-	-	-	-	-	-	-
Residual crack width	-	-	-	-	-	-	-	-
The minimum drift	0.27%	-0.28%	0.64%	-0.75%	0.76%	-1.50%	-	-

PCa14	Serviceability limit state		Reparability limit state I		Reparability limit state II		Safety limit state	
	Positive	Negative	Positive	Negative	Positive	Negative	Positive	Negative
Longitudinal mild reinforcement	1.98%	-3.07%	-	-	-	-	-	-
Unbonded PS tendons			1.51%	-1.21%	2.98%	-2.82%	-	-
Concrete	0.86%	-0.75%	0.75%	-1.00%	1.50%	-1.55%	-	-
Residual drift ratio	-	-	-	-	-	-	-	-
Residual crack width	-	-0.75%	-	-	-	-	-	-
The minimum drift	0.86%	-0.75%	0.75%	-1.00%	1.50%	-1.55%	-	-

PCa15A	Serviceability limit state		Reparability limit state I		Reparability limit state II		Safety limit state	
	Positive	Negative	Positive	Negative	Positive	Negative	Positive	Negative
Longitudinal mild reinforcement	1.46%	-1.50%	-	-	-	-	-	-
Unbonded PS tendons			1.61%	-1.39%	-	-	-	-
Concrete	0.52%	-0.44%	0.89%	-1.00%	1.47%	-1.51%	-	-
Residual drift ratio	-	-	-	-	-	-	-	-
Residual crack width	-	-	-	-	-	-	-	-
The minimum drift	0.52%	-0.44%	0.89%	-1.00%	1.47%	-1.51%	-	-

PCa15B	Serviceability limit state		Reparability limit state I		Reparability limit state II		Safety limit state	
	Positive	Negative	Positive	Negative	Positive	Negative	Positive	Negative
Longitudinal mild reinforcement	1.92%	-1.88%	-	-	-	-	-	-
Unbonded PS tendons			2.30%*	-2.19%*	-*	-3.67%*	-	-
Concrete	0.50%	-0.50%	0.75%	-0.99%	2.00%	-3.06%	-	-
Residual drift ratio	-	-	-	-	-	-	-	-
Residual crack width	-	-	-	-	-	-	-	-
The minimum drift	0.50%	-0.50%	0.75%	-0.99%	2.00%	-3.06%	-	-

\*Strain of PS tendon was not measured, therefore, yielding point was estimated using force data measured by a load cell.

### 3. Conclusions

An experimental study was conducted to evaluate the structural performance and damage for unbonded prestressed precast concrete members. The findings of this study are summarized:

1. The Shear force versus drift angle responses of all specimens had small residual drift angle and S-shape hysteresis behavior which has small amount of energy dissipation.
2. Compressive yielding of longitudinal mild reinforcement was observed in several specimens before the peak load. It is necessary to consider compressive stress of longitudinal mild reinforcement for moment calculation.
3. Damage evaluation shows effective prestressing force ratio is one of important factors in order to control damage in design for unbonded prestressed concrete beams.



4. The drift angle at serviceability limit state ranged from  $R=0.5\%$  to  $R=1.0\%$  except for PCa13 which has high effective prestressing force ratio. All specimens did not reach safety limit state until  $R=4\%$ . Thus, excellent low damage performances of unbonded prestressed concrete beams were confirmed.

#### 4. Acknowledgements

The research was funded by the promotion of building standard provisions by the Ministry of Land, Infrastructure, Transportation and Tourism in 2012 and 2013. The authors acknowledge the committee members of the Association of New Urban Housing Technology for valuable comments. The efforts of graduate students (Mr. S. Sinthaworn) who contributed the project are highly appreciated.

#### 5. References

- [1] Priestley, M.J.N. (1991): Overview of the PRESSS Research Program. *PCI Journal*, 36(4), 50-57.
- [2] Priestley, M.J.N. (1996): The PRESSS Program Current Status and Proposed Plans for Phase III. *PCI Journal*, 41(2), 22-40.
- [3] Priestley, M.J.N., Sritharan, S., Conley, J.R. and Pampanin, S. (1999): Preliminary Results and Conclusions from the PRESSS Five-Storey Precast Concrete Test-Building. *PCI Journal*, 44(6), 42-67.
- [4] Englekirk, R.E. (2002): Design-Construction of the Paramount - A 39-story Precast Prestressed Concrete Apartment Building. *PCI Journal*, 47(4), 56-71.
- [5] Marriott, D., Pampanin, S. and Palermo, A. (2008): Quasi-static and pseudo-dynamic testing of unbonded post-tensioned rocking bridge piers with external replaceable dissipaters. *Earthquake Engineering and Structural Dynamics*, DOI: 10.1002/eqe.857, www.interscience.wiley.com
- [6] Moriguchi, Y., Watanabe, H., Gioia, G. and Kono, S. (2014): An experimental study on flexural behavior for prestressed concrete beams post-tensioned with unbonded tendons with slab. *JPCI*, 161-166. (in Japanese)
- [7] Architectural Institute of Japan (2015): Guidelines for structural design and construction of prestressed concrete buildings based on performance evaluation concept (draft), *Architectural Institute of Japan* (in Japanese)